

A Cross Scanning Crack Damage Quantitative Monitoring and Imaging Method

Zi Wang, Shaodong Zhang, Yehai Li, Qiang Wang, Zhongqing Su, Dong
Yue

Submitted to *IEEE Transactions on Instrumentation and Measurement* on 28 Feb 2022. This work was supported by the China Postdoctoral Science Foundation (Grant No. 2015M570401) (*Corresponding author: Qiang Wang*)

Zi Wang, Shaodong Zhang, Qiang Wang and Dong Yue are with College of Automation & College of Artificial Intelligence, Nanjing University of Posts and Telecommunications, Nanjing, China (e-mail: wangqiang@njupt.edu.cn).

Yehai Li is with Shenzhen Key Laboratory of Smart Sensing and Intelligent Systems, Shenzhen Institute of Advanced Technology, Chinese Academy of Sciences, Shenzhen 518055, P.R. China.

Zhongqing Su is with the Department of Mechanical Engineering, The Hong Kong Polytechnic University, Kowloon, Hong Kong SAR, China.

Abstract —Quantitative crack monitoring and detection is one of the focuses of attention in structural health monitoring, due to its concealment and harmfulness. However, the existing guided wave and PZT sensor array based structural health monitoring approaches often ignore the crack orientation information which is the key issue in the crack monitoring, so that it is hard to effectively evaluate the crack damage. In this study, the circular piezoelectric array and active Lamb wave RAPID imaging technology are introduced and improved to study the quantitative monitoring of crack damage. A cross scanning method is proposed to determine the crack orientation, based on the different degree of response signal variation on monitoring path with different angles. Accordingly, the signal difference coefficient (SDC) value of the detected monitoring path of parallel or approximate parallel crack damage is corrected to strengthen the reconstruction information of crack orientation. After that, the image reconstruction and quantitative evaluation of crack damage can be realized by the enhanced SDC information. Several experiments were carried out on the aluminum plate to validate the proposed method. The cracks in different positions and orientations were monitored and evaluated by the proposed method. The experimental results showed that the crack orientation can be identified well by the proposed cross scanning crack monitoring and imaging method.

Index Terms—crack damage, circular array, Lamb wave, quantitative monitoring, cross scanning method

I. INTRODUCTION

Engineering structures in aerospace, high-speed rail and other fields, which usually run under long-term and alternating loads, are easy to introduce structural damages such as cracks. In order to ensure operation safety, it is necessary to evaluate these structures' integrity regularly. On one hand, the off-line structural integrity testing such as non-destructive testing inevitably reduces the service efficiency of the equipment. On the other hand, it is unable to monitor the structural safety during the operation, especially the metal crack damage which is usually hidden and difficult to find intuitively. Therefore, the on-line monitoring and quantitative evaluation of structural crack damage is of great significance to ensure structural safety and improve maintenance efficiency.

Lamb wave is a special kind of ultrasonic wave. Due to its low attenuation characteristics in the plate structure and high sensitivity to small damages, Lamb wave based structural damage monitoring and evaluation is a research hotspot in the field of structural health monitoring, which has attracted extensive attention [1-5]. The occurrence of damage can be determined by comparing the response signals before and after the structure damaged [6]. Most researches have been focusing on the evaluation of crack length and the trend of crack extension [7-10]. It is well known when Lamb waves propagate across cracks, there will be different degrees of reflection, scattering and endpoint effect, resulting in the change of Lamb wave mode and waveform [11-12]. The above signal changes provide a lot of information for

damage monitoring. The crack monitoring methods usually establish the relationship between crack length and signal features, such as wavelet transform [13], time of flight (*ToF*) [14-15], probability reconstruction algorithm [16-17]. In addition, some advanced algorithms, such as Bayesian method [18] and particle filter [19], have been used to predict the trend of crack growth. However, most of the researches focus on the evaluation of the crack length that under the premise of the known crack orientation, while the damage monitoring and evaluation of the unknown crack direction is rarely studied. In practical engineering applications, the occurrence and location of structural crack damage are unknown, and the crack orientation is also uncertain. Therefore, the above methods are far from the real world applications.

Since the incident angle of Lamb wave signal propagating through the crack varies with the occurrence and development of the crack and the subsequent propagation of the signal is also affected by the crack, it leads to different signal difference coefficients between the nondestructive structural response and the damaged structural one. Thus, it is expected to achieve crack damage at any position and angle. Based on the above ideas, the cross scanning method is proposed in this paper to detect the orientation of cracks, and then obtains the reconstruction image and evaluation of structural cracks, which provides the necessary data support for structural health assessment.

II. LAMB WAVE PROPATION AND THE DETECTION MECHANISM FOR CRACK

DAMAGE

A. Basic theory of Lamb wave

The longitudinal wave and the transverse wave are coupled to form the elastic wave in the plate that is Lamb wave. When Lamb wave propagates in the medium, it is divided into symmetric mode and anti-symmetric mode, according to the trajectory of particle vibration in plate.

$$\frac{\tan(qh/2)}{\tan(ph/2)} = -\frac{4k^2pq}{(q^2-k^2)^2} \quad \text{symmetric mode} \quad (1)$$

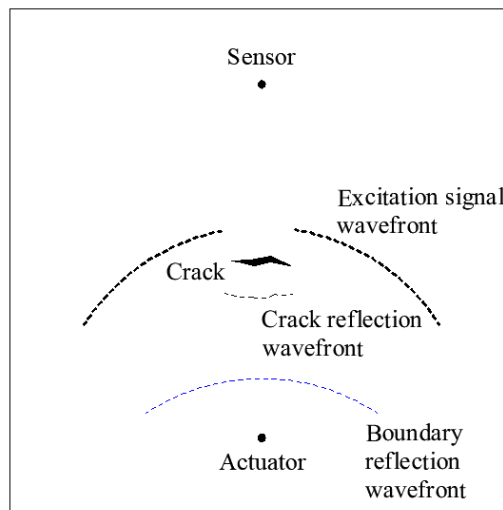
$$\frac{\tan(qh/2)}{\tan(ph/2)} = -\frac{(q^2-k^2)^2}{4k^2pq} \quad \text{anti-symmetric mode} \quad (2)$$

$p^2 = \frac{\omega^2}{c_l^2} - k^2$, $q^2 = \frac{\omega^2}{c_t^2} - k^2$, $k = \frac{\omega}{c_p}$, $\omega = 2\pi f$, ω is the angular frequency, h is the plate thickness; c_l is the velocity of P-wave; c_t is the velocity of S-wave; c_p is the phase velocity of Lamb wave[20].

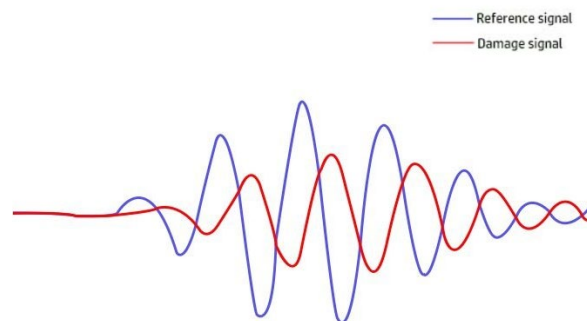
According to formulas (1) and (2), the wave velocity of Lamb wave symmetric model is a function of the product of frequency and thickness. Due to equations have numerous roots, a variety of propagation modes can be obtained, which are symmetric mode (S0, S1,...) and anti-symmetric mode (A0, A1,...). Multimodal signal is complex, which brings difficulty to signal analysis. Therefore narrowband signal can be used as excitation signal to adjust the center frequency and select the appropriate excitation frequency [21].

B. Analysis of lamb wave propagation influenced by crack

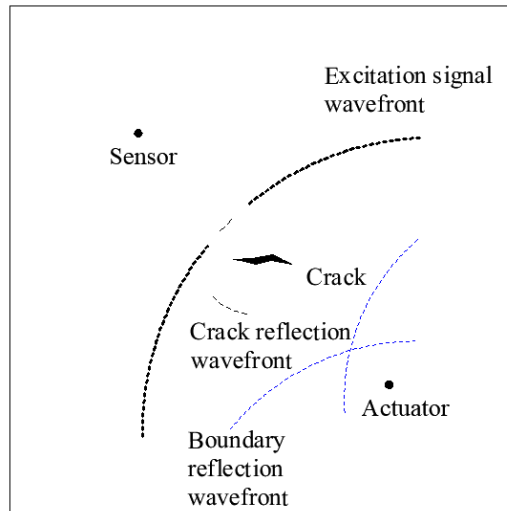
The changes of Lamb wave signal propagation caused by structural crack damage can be analyzed through the finite element simulation under ABAQUS environment. As shown in Figure 1, when the signal passes through the crack, there will be signal reflection, scattering and other phenomena, resulting in energy attenuation.



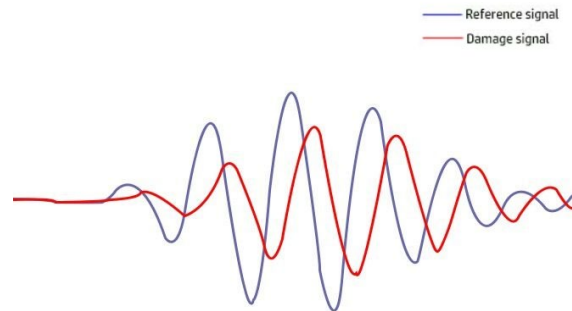
(a) Normal incidence wave to crack orientation



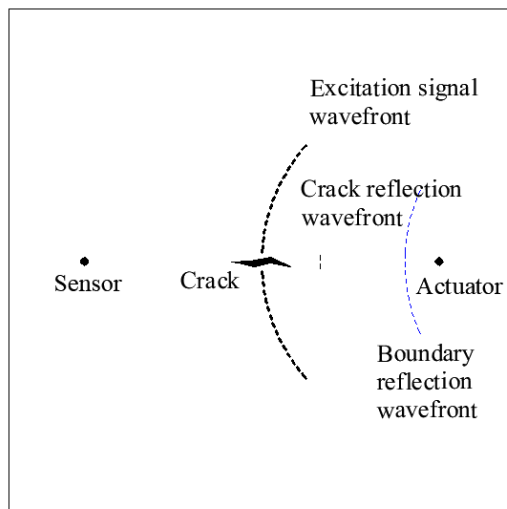
(b) Structural response signal perpendicular to the crack



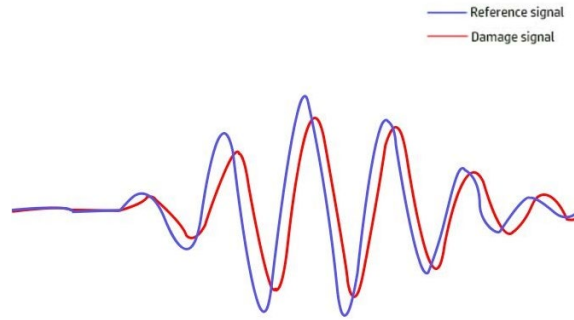
(c) Oblique incidence wave to crack orientation



(d) Structural response signal inclined to the crack



(e) Parallel incidence wave to crack orientation



(f) Structural response signal parallel to the crack

Figure 1. Monitor signal propagation

In order to verify the influence of the excitation monitoring signal passing through crack under different angles, a 600mm * 600mm * 3mm plate model is established with exciting monitoring signal from three different orientations. As shown in Figure 1 (a) and (b), when the monitoring path is perpendicular to the crack damage, the single-mode signal excited at Actuator will form the maximum reflected signal field. As shown in Figure 1 (c) and (d), when the monitoring signal is oblique to the crack damage, part of the signal reflection occurs and the transmitted signal wave field expands. As shown in Figure 1 (e) and (f), when the excitation signal is parallel to the crack damage, little signal reflection occurs, and most of the sound field signal can be received at Sensor. According to these analyses, the reflected sound field and the transmitted sound field hold different energy and range when the monitoring signal is incident in different orientations. Considering that the occurrence and location of structural crack damage are unknown, the occurrence and evaluation of damage can be determined by scanning. Therefore, it is necessary to research and design the

piezoelectric actuator/sensor array layout, damage information capture method and damage evaluation method.

III. PRINCIPLE OF QUANTITATIVE CRACK MONITORING METHOD

A. Basic idea of crack location and orientation determination

Through the correlation analysis of the response signals before and after the structural damage happen, signals change caused by the damage defects can be extracted. The probability of damage defect at any point in the structure can be reconstructed by the change between the damage signal and the health signal and the distance from the point to the sensing path. When the monitoring signal propagates along the crack orientation, the effect on monitoring signal is little, so the information of the crack orientation is bound to be lost. Considering that the crack propagation to a certain extent will affect the signal propagation, it is difficult to objectively judge the orientation of the crack from the changes of monitoring signal on a single path. Due to the situation of signal propagation in the monitoring path parallel to the crack orientation, the largest signal change is in the intersecting paths of vertical crack incidence and parallel crack incidence, and the crack orientation can be accurately determined. Therefore, the propagation path along the crack orientation can be found by using combination of two cross monitoring paths to scan the crack area. The orientation of crack damage can be determined, and the evaluation of crack damage length can be realized by correcting the probability of damage defects in the propagation path and making up the missing information of crack orientation. In order

to achieve this goal, we will design the method from three aspects: the design of piezoelectric array, the determination of crack cross scanning and the evaluation of damage imaging.

B. the design of piezoelectric array

In order to collect excitation and monitoring signal, lead zirconate titanate piezoelectric element (PZT) is used as sensor in the experiment. Excitation sensing methods can be divided into pulse echo and pitch catch [22-24]. Pulse echo method is adverse to determine the orientation of crack damage [14], so pitch catch method is used for monitoring. Distributed array and circular array are commonly use [25-27]. In real life, due to the shape of crack damage is small and the crack orientation can be any angle, it is necessary to detect the damage from all orientations. Therefore, the circular array is used in the experiment, as shown in Figure 2.

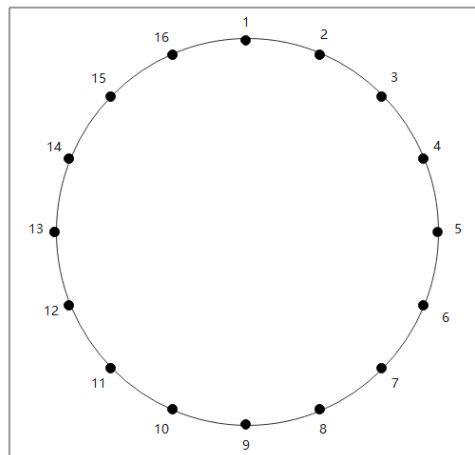


Figure 2. Circular array

C. the monitoring process of cross scanning crack

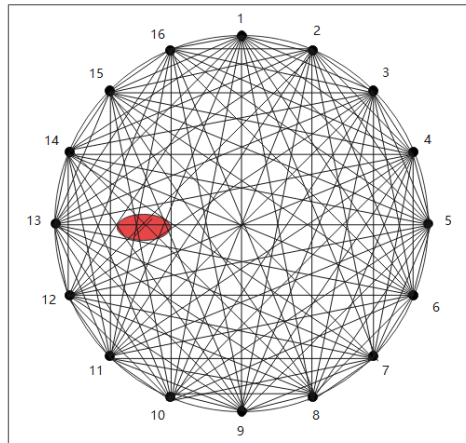
In order to show the strength of energy attenuation, the statistical difference between damage and non-destructive signal can be expressed by signal difference coefficient

(SDC)[28]. The definition of SDC value is as follow:

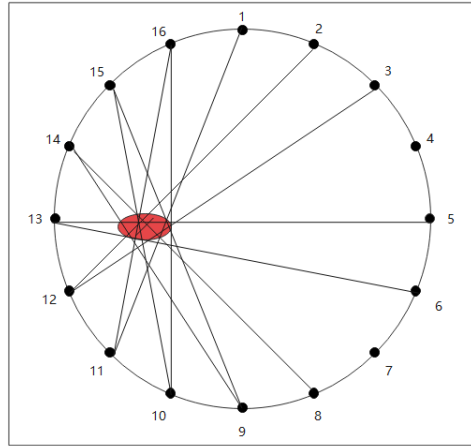
$$SDC_{ij} = 1 - \left| \frac{\int_{t_0}^{t_0+\Delta t} [x_{ij}-\mu_x][y_{ij}-\mu_y]dt}{\sqrt{\int_{t_0}^{t_0+\Delta t} [x_{ij}-\mu_x]^2 dt \int_{t_0}^{t_0+\Delta t} [y_{ij}-\mu_y]^2 dt}} \right| \quad (3)$$

In the formula (3): i is the actuator and j is the sensor; x_{ij} and y_{ij} are non-destructive and damage signals; t_0 is the direct time of the excitation signal in each monitoring path; μ_x and μ_y are the average value of the non-destructive and damage signal; Δt is a time window.

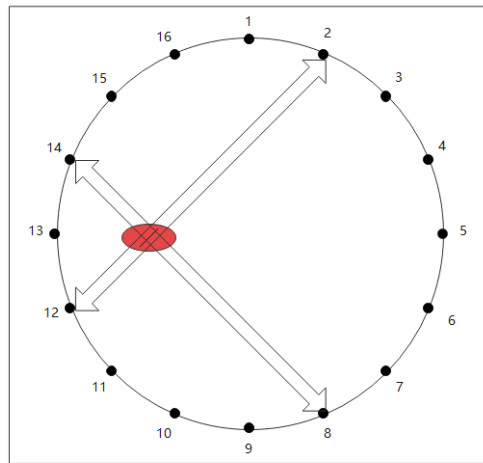
From the previous finite element simulation, When the excitation signal is vertical to the crack, the reflection of the excitation signal and the change of the SDC value of the path are large; When the excitation signal is parallel to the crack, the influence of the crack on the excitation signal and the change of SDC value of the path are small. Therefore, the difference of SDC on the damage path perpendicular to each other will be the largest. So, the problem of finding the crack orientation is transformed into finding the largest SDC difference in the combination of cross paths. For the unknown crack, the above process can be described as cross scanning.



(a) Scan all the monitoring path



(b) Determine the damage area



(c) The largest SDC difference of cross paths

Figure 3. Schematic diagram

As shown in Figure 3, the excitation end is using PZT No. 1 # - 16 # for data collection in turn. Then, calculating the SDC value of each path to determine whether the monitoring path passes through the crack, when SDC value exceeds a certain threshold value (the threshold value is caused by the signal change under the interference), crack damage can be determined in the path. In the path through the damage, finding all combinations of vertical cross path, and calculating the absolute value of SDC difference of these combinations to complete the cross scanning of

crack damage.

The process of crack monitoring at any angle is divided into the following steps

(1) According to the size of the plate structure, arrange PZT sensors by the circular array.

(2) One PZT in the circular array is used as the excitation end A_i , and the other sensors S_j ($j \in [1,16]$, and $j < i$) are used as the receiving end to collect the response signal of Lamb wave.

(3) Using all PZT in the sensor array as the excitation end in turn, repeat step (2), collecting data and calculating the SDC value of all paths of excitation-sensing.

(4) Through the threshold to determine the suspected damage path, the cross scanning method is used to scan the damage area of the reconstructed image, calculating the difference of SDC values of all suspected vertical paths, then finding the largest absolute value of the cross path, and the low SDC value in the path is the crack orientation.

D. Crack imaging

Reconstructing the probability distribution diagram of damage after calculating the SDC value of each monitoring path. According to the principle of probability damage distribution [26], establishing the ellipse weight model. The probability distribution of damage defect at any point (x, y) in the structure is shown in Figure 4. The weight is assigned according to the distance from any point in the ellipse to the actuator and the

sensor. The actuator and the sensor are the areas with the largest weight, and the ellipse edge weight is 0. The deeper the color, the higher the damage probability.

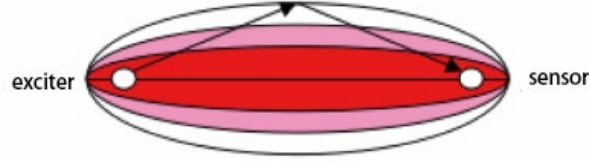


Figure 4. Ellipse weight model

According to formula (4), the range of signal difference coefficient is $[0,1]$. The SDC value of the monitoring path also reflects the degree of damage. If the signal is completely uncorrelated, the SDC value is 1, which means the monitoring path has seriously damage; if the signal is completely correlated, the SDC value is 0, the monitoring path is healthy. Due to the SDC value of the path parallel to the crack is small, correcting the SDC value to 1. After correction, the SDC formula is shown in formula (4).

$$SDC_{ij} = \begin{cases} 1, & \text{The path } ij \text{ is the crack direction} \\ 1 - \left| \frac{\int_{t_0}^{t_0+\Delta t} [x_{ij}-\mu][y_{ij}-\mu] dt}{\int_{t_0}^{t_0+\Delta t} [x_{ij}-\mu]^2 dt \int_{t_0}^{t_0+\Delta t} [y_{ij}-\mu]^2 dt} \right|, & \text{others} \end{cases} \quad (4)$$

According to the weight distribution of each path and stack the weight, the weight of damage defect at any point (x, y) in the structure is:

$$p(x, y) = \sum_{i=1}^{N-1} \sum_{j=i+1}^N SDC_{ij} s_{ij}(x, y) \quad (5)$$

Here, N is the total of damage paths in the sensor array. $s_{ij}(x, y)$ is the spatial distribution function, the expression is as follows:

$$\begin{cases} s_{ij}(x, y) = \frac{\beta - R_{ij}(x, y)}{1 - \beta}, & \beta > R_{ij}(x, y) \\ s_{ij}(x, y) = 0 & , \quad \beta \leq R_{ij}(x, y) \end{cases} \quad (6)$$

In formula (6): β is used to control the eccentricity of ellipse, and the value is bigger than 1. It is taken the value as 1.05 in experiments[29]. $R_{ij}(x, y)$ is the ratio of the distances from point (x, y) to actuator (x_{ik}, y_{ik}) and sensor (x_{jk}, y_{jk}) and the distance from actuator (x_{ik}, y_{ik}) to sensor (x_{jk}, y_{jk}) .

$$R_{ij}(x, y) = \frac{\sqrt{(x-x_{ik})^2+(y-y_{ik})^2} + \sqrt{(x-x_{jk})^2+(y-y_{jk})^2}}{\sqrt{(x_{ik}-x_{jk})^2+(y_{ik}-y_{jk})^2}} \quad (7)$$

IV. EXPERIMENTAL VERIFICATION

A. Experimental setup

The test object was using aluminum sheet. (600mm * 600mm * 3mm Young's modulus: 71GPa, density: 2711kg/m³). The experiment takes the geometric center to arrange the circular array by 16 PZTs (1 # - 16 #) under the radius of 210mm. The damping of local structure in the tested specimen can be changed by pasting different specifications of metal blocks [30], simulating the influence of cracks in the structure. Due to the dispersion characteristics of Lamb wave, multi-mode will increase the difficulty of signal analysis. According to the experimental measurement, the Hanning window function was used to modulate the narrow-band excitation signal [14] which is under the center frequency of 200kHz, and the experimental equipment is shown in Figure 5. The monitoring system is consisted of power amplifier and charge amplifier, which are used to amplify the excitation and the sensing signal. NIUSB-6366 data acquisition card is used to transmit and receive signals.

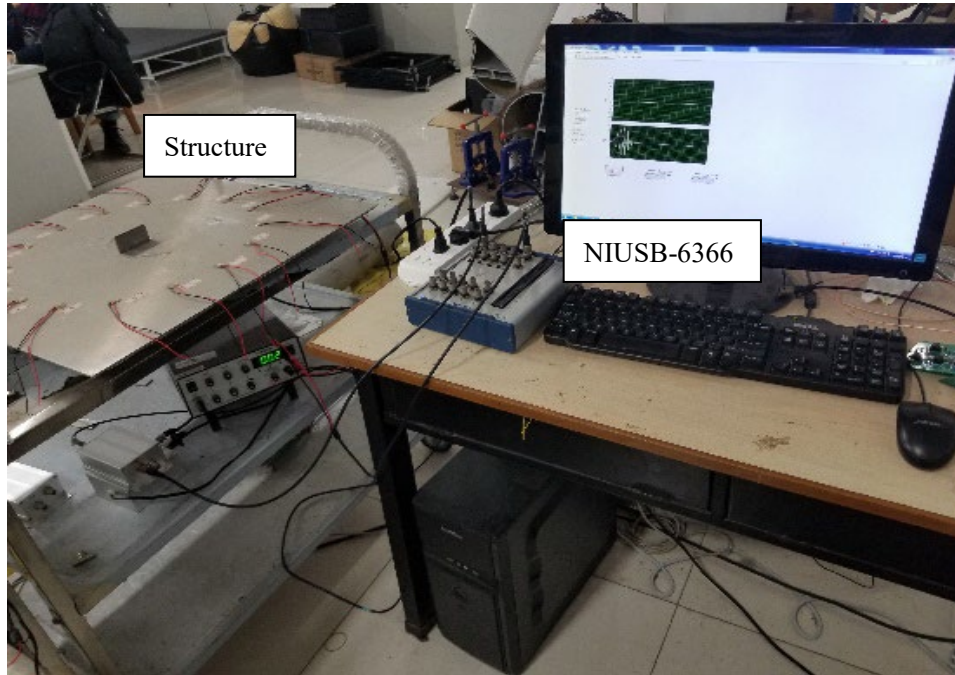


Figure 5. Experimental setup

B. Experimental data analysis

The experimental verification is divided into two parts: one is to verify the influence of the excitation monitoring signal passing through crack under different angles. The other is to verify the imaging of cross scanning method through three groups of simulated damage experiments under different specifications and orientations.

(1)As shown in Figure 6, simulated crack (60mm * 3mm) is located on the monitoring path. The excitation signals pass through the crack in three orientations: vertical, inclined and parallel, and three structural response signals of typical sensing paths were obtained.

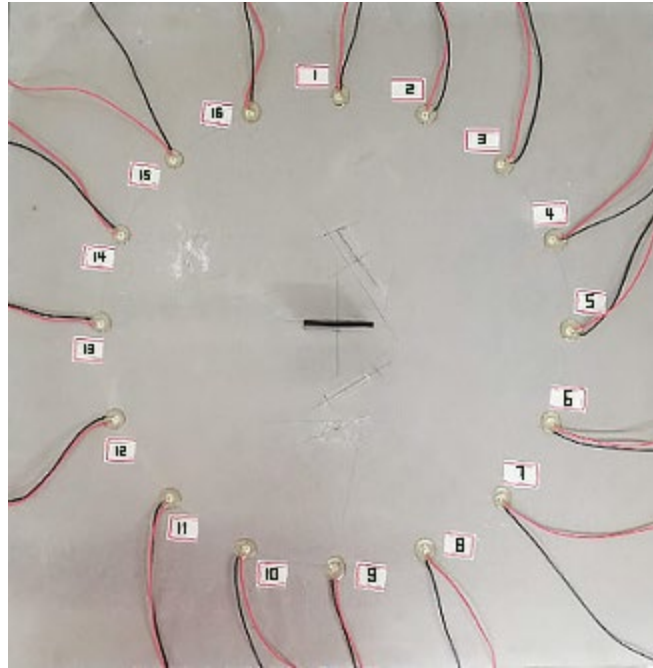


Figure 6. 60mm crack damage

The SDC values of three typical sensing paths are shown in Figure 7, and the structural response signals are shown in Figure 8. In the path A_1S_9 (1 # 9 #, A is the actuator, S is the sensor, and the subscript is the number of PZT), the difference between the reference signal and the damage signal is the largest. The amplitude of the damage signal is in large decrease. In the path A_5S_{13} (5 # 13 #), the difference between the reference signal and the damage signal is the smallest. The amplitude of the damage signal is in low decreased. These also verify the conclusion of the above simulation.

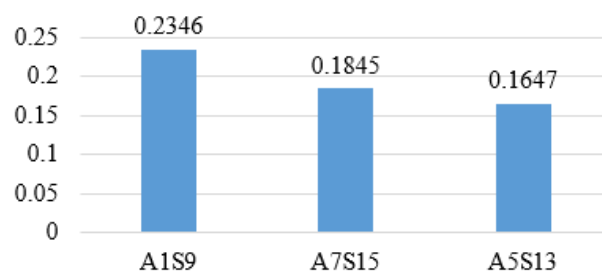
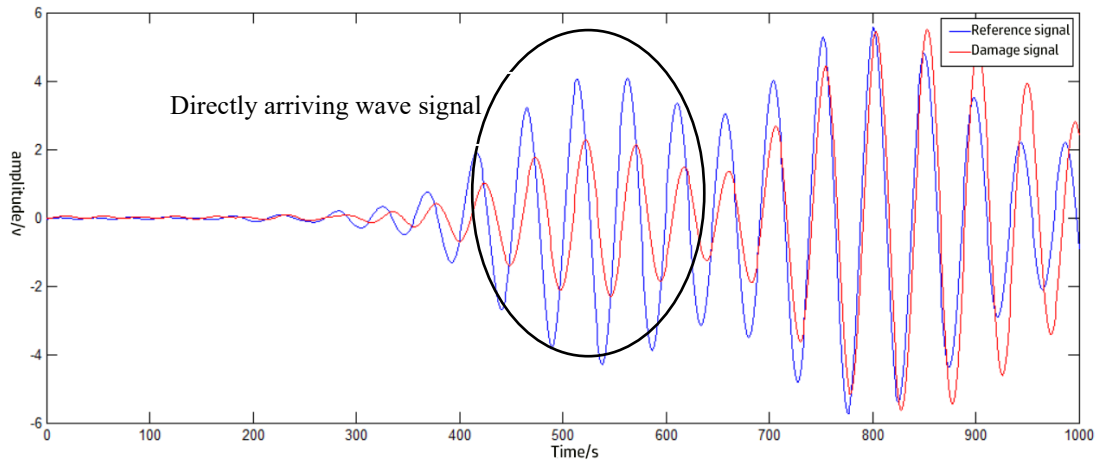
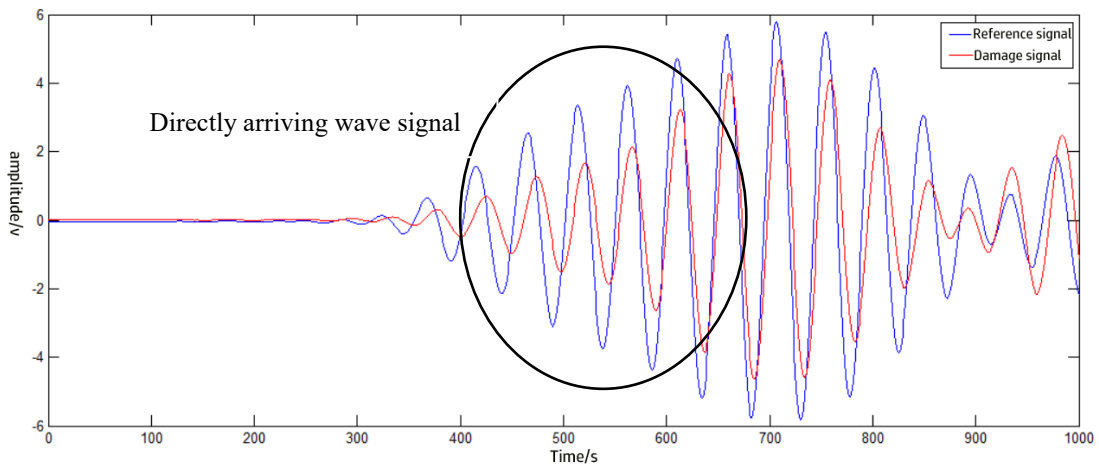


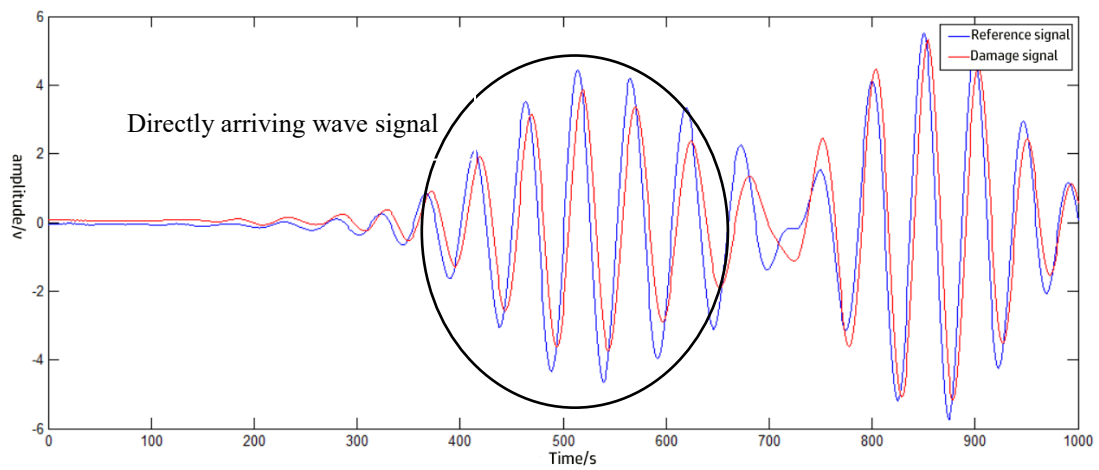
Figure 7. Three sets of path SDC values



(a) Response signal with A1S9 perpendicular to the crack



(b) Response signal of A7S15 inclined to crack



(c) Response signal of A5S13 parallel to the crack

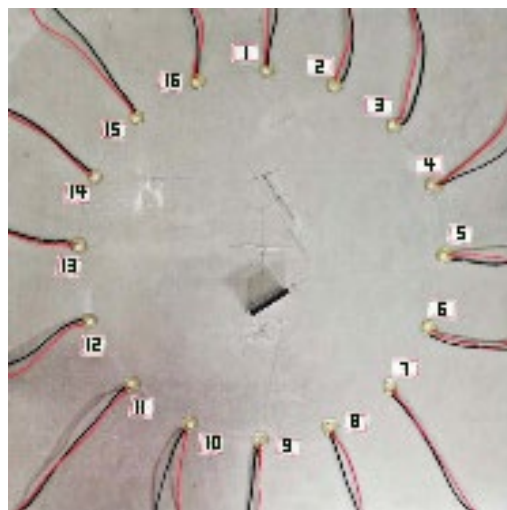
Figure 8. Three groups of typical structural response signals

(2) Due to crack orientation and length are different, designing three groups of experiments, the crack size of three groups is shown in Table 1.

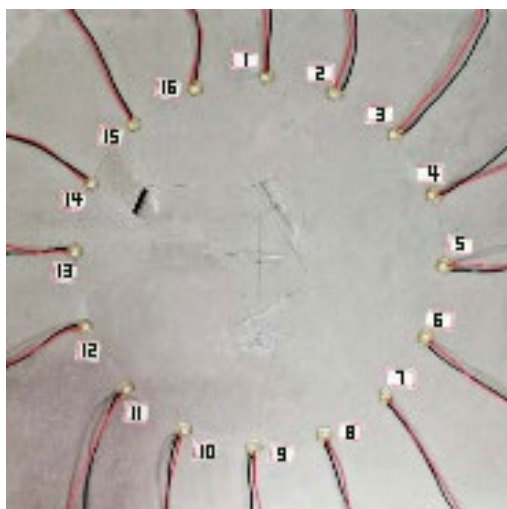
Table 1. Three sets of experimental specifications

	Exp1	Exp2	Exp3
angle	30°	68°	125°
length	50mm	30mm	70mm

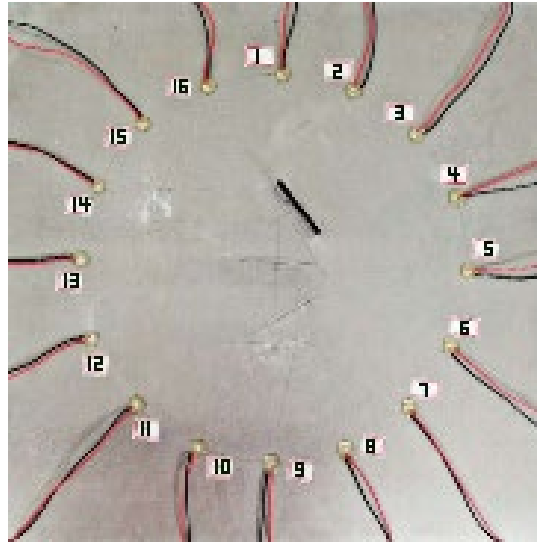
The damage of the three experimental groups is shown in Figure 9.



(a) Experiment 1



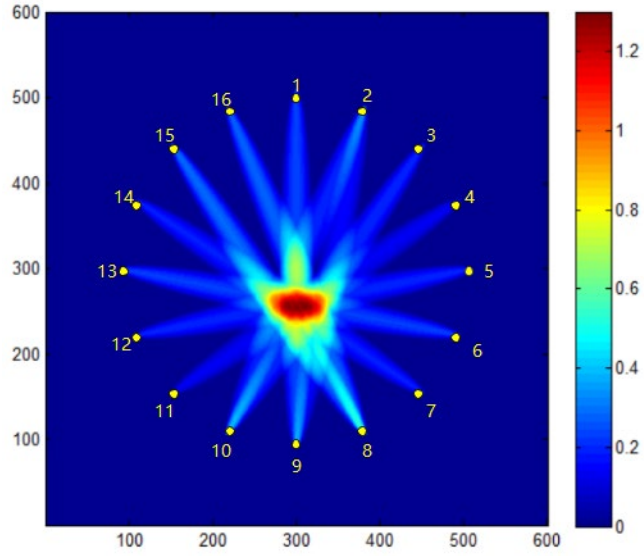
(b) Experiment 2



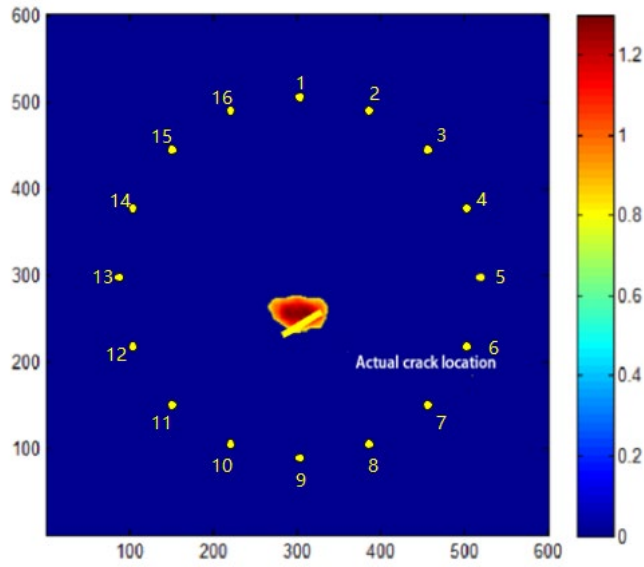
(c) Experiment 3

Figure 9. The location of the three groups of experimental damage

Each experiment collects 120 sets of signals. The traditional RAPID tomography method is used to image the crack damage in the plate, and the results are shown in Figure 10. The traditional method locate the damage roughly, and can not accurately monitor the crack orientation. Through the cross scanning method to scan the suspected damage path, the absolute value of cross path difference in Experiment 1 is shown in Figure 11, in which the SDC of path A_4S_{11} is 0.1426, and the SDC of path A_8S_{15} is 0.2853. The absolute value of SDC difference between the cross paths is the largest, and it is significantly larger than other. According to the cross scanning method, the path A_4S_{11} is the orientation of the crack. After correcting the SDC of the monitoring path which is parallel or approximately parallel to cracks, the imaging results are shown in Figure 12.



(a) Imaging before thresholding



(b) Thresholding imaging

Figure 10. Traditional RAPID imaging in Experiment 1

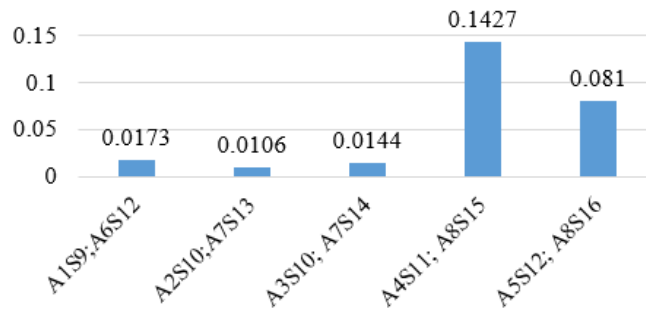
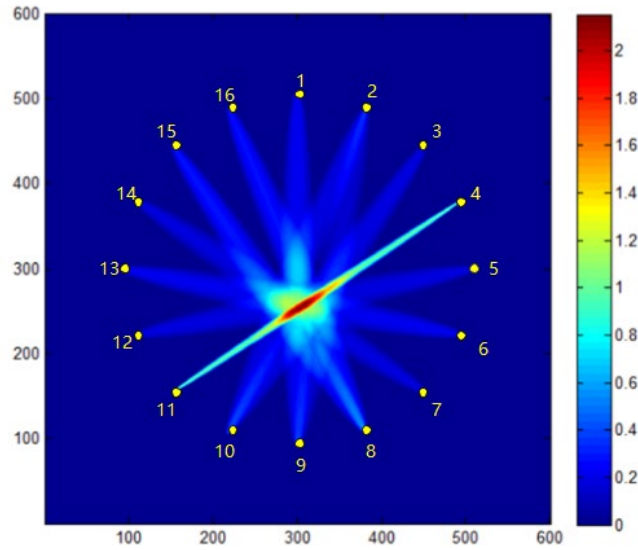
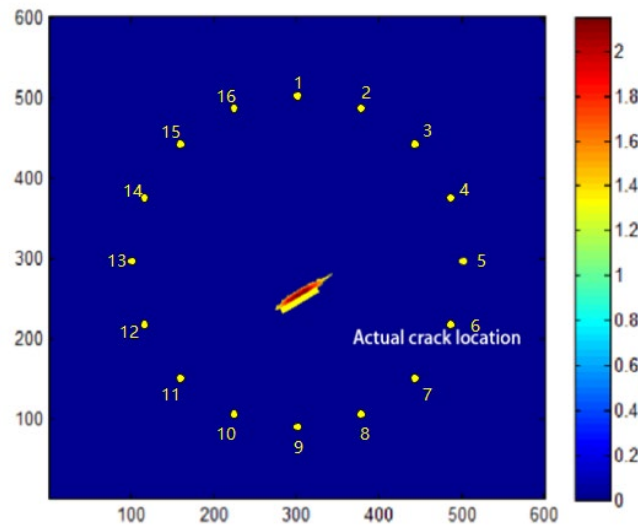


Figure 11. The absolute value of the difference of the orthogonal path in Experiment 1



(a) Imaging before thresholding

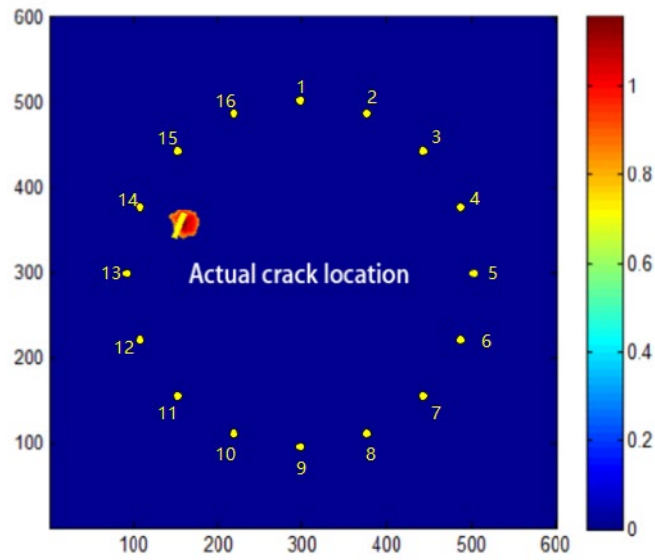


(b) Thresholding imaging

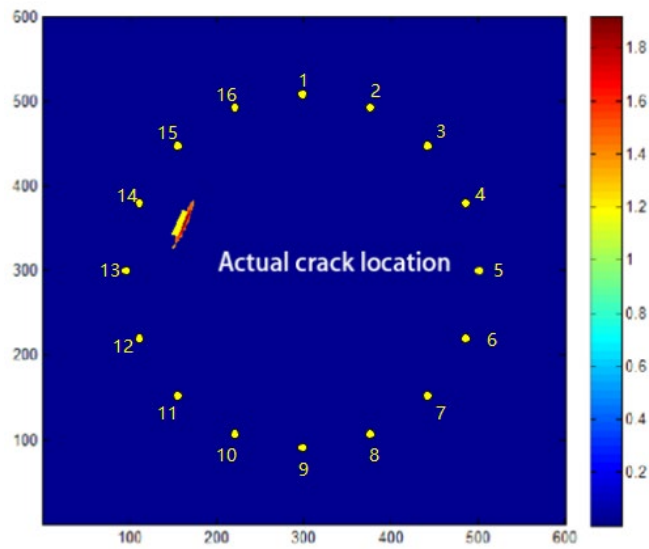
Figure 12. Cross Scanning Method Imaging in Experiment 1

In Experiment 2, the traditional RAPID tomography method is used to image the crack damage in the plate. After threshold, the results are shown in Figure 13 (a). The suspected damage path is scanned by the cross scanning method, after the SDC of the monitoring path under parallel or approximately parallel to crack is corrected, the imaging result is shown in Figure 13 (b). The absolute value of cross path difference in Experiment 2 is shown in Figure 14. In Experiment 2, the SDC of crossing path

A_6S_{14} is 0.2808, and path $A_{12}S_{16}$ is 0.1774. According to the cross scanning method, path $A_{12}S_{16}$ is the orientation of crack.



(a) Traditional RAPID imaging



(b) Cross Scanning Method Imaging

Figure 13. Imaging results in Experiment 2

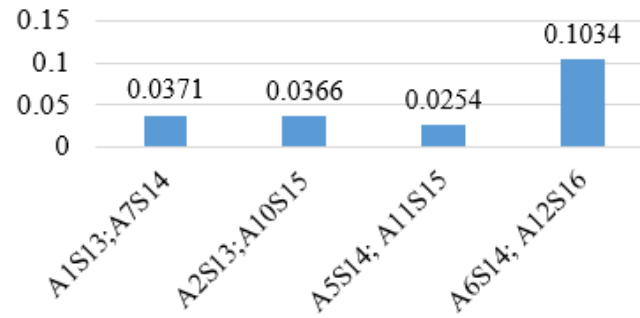
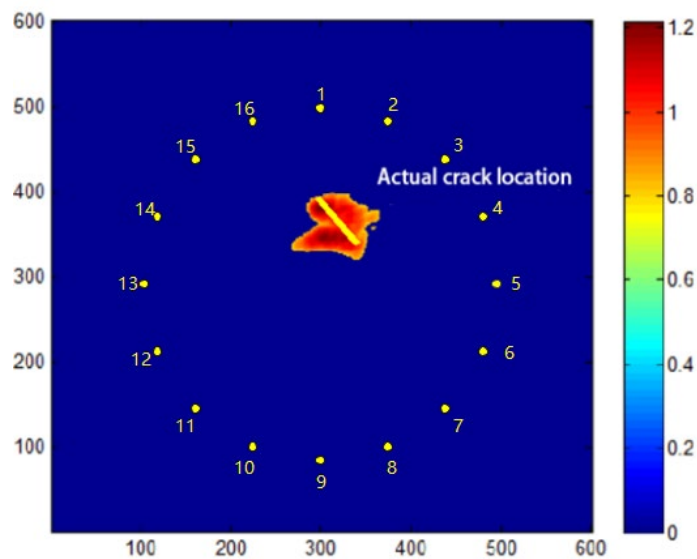
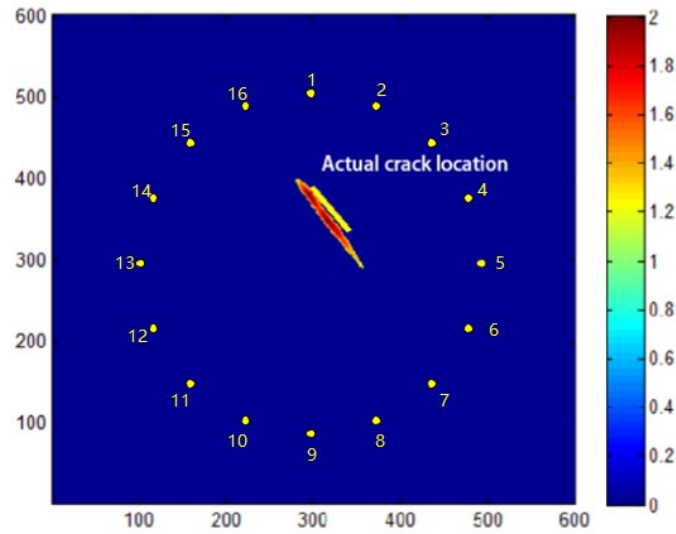


Figure 14. The absolute value of the difference of the orthogonal path in Experiment 2

In Experiment 3, the traditional RAPID tomography method is used to image the crack damage in the plate. After threshold, the results are shown in Figure 15 (a). The suspected damage path is scanned by the cross scanning method, after the SDC of the monitoring path of parallel or approximately parallel to crack is corrected, the imaging result is shown in Figure 15 (b). The absolute value of cross path difference in Experiment 3 is shown in Figure 16. In Experiment 3, the SDC of crossing path A₃S₁₂ is 0.3318, and path A₇S₁₆ is 0.1754. According to the cross scanning method, path A₇S₁₆ is the orientation of crack.



(a) Traditional RAPID imaging



(b) Cross Scanning Method Imaging

Figure 15. Imaging results in Experiment 3

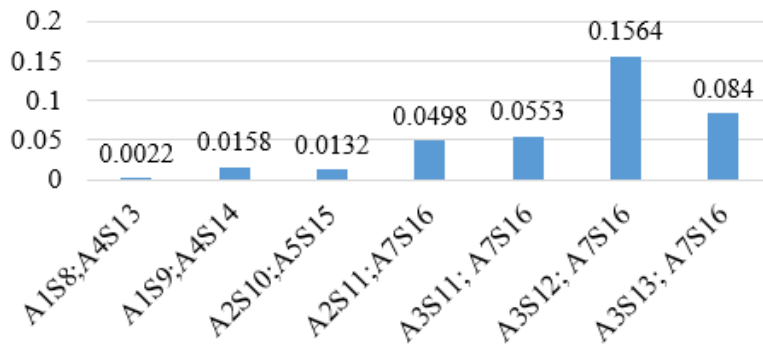


Figure 16. The absolute value of the difference of the orthogonal path in Experiment 3

The results of Experiment 1 and Experiment 2 show that the reconstructed crack is very close to the actual crack. The error in Experiment 3 is slightly large. The angle between the reconstructed crack and the positive orientation of x-axis is 126 °C, and the angle between the actual crack and the positive orientation of x-axis is 133 °C. The reconstruction error is - 7 °C. The error is affected by the sensor spacing in the sensor array, so the weight is assigned to the sensor path. Compared with the traditional RAPID algorithm, Cross Scanning Method can determine the crack

orientation by analyzing the influence of the monitoring signal passing through the unknown crack.

V. CONCLUSION

The Lamb wave quantitative imaging monitoring and evaluation method of crack under arbitrary angle is studied. ABAQUS finite element simulation is used to judge the influence of crack on incident signal. When the excitation signal is vertical to the crack, the reflection of the excitation signal are large. In the experiment, the circular array is used, the cross scanning method is introduced to identify the orientation of crack, and the traditional RAPID algorithm is improved to reconstruct the image of crack damage. The experimental results on aluminum plate show that: (1) The above method can effectively determine the orientation of cracks; (2) In terms of quantitative monitoring, compared with the traditional RAPID algorithm, the improved imaging has good consistency with the actual damage, which can be used for crack damage monitoring. In the follow-up research, we will study how to judge the position and direction of multiple cracks in the structure.

REFERENCES

1. M. Y. Bhuiyan, Y. Shen and V. Giurgiutiu, "Interaction of Lamb waves with rivet hole cracks from multiple directions," *Proc. Inst. Mech. Eng. Part C, J. Mech. Eng. Sci.*, vol. 231, no. 16, pp. 2974-2987, 2017, doi: 10.1177/0954406216686996.

2. P. Kudela, M. Radziński, et al, "Structural health monitoring system based on a concept of Lamb wave focusing by the piezoelectric array," *Mech. Syst. Signal Process.*, vol. 108, pp. 21-32, 2018, doi: 10.1016/j.ymssp.2018.02.008.
3. J. K. Agrahari and S. Kapuria, "Active detection of block mass and notch-type damages in metallic plates using a refined time-reversed Lamb wave technique," *Struct. Control Health Monit.*, vol. 25, no. 2, pp. 1-18, 2018, doi: 10.1002/stc.2064.
4. A. Stawiarski, M. Barski, and P. Pająk, "Fatigue crack detection and identification by the elastic wave propagation method," *Mech. Syst. Signal Process.*, vol. 89, no. 15, pp. 119-130, 2017, doi: 10.1016/j.ymssp.2016.08.023.
5. F. Zonzini, C. Aguzzi, et al., "Structural Health Monitoring and Prognostic of Industrial Plants and Civil Structures: A Sensor to Cloud Architecture," *IEEE Trans. Instrum. Meas.*, vol. 23, no. 9, pp. 21-27, 2020, doi: 10.1109/MIM.2020.9289069.
6. Y. K. An, J. H. Kim and H. J. Yim, "Lamb wave line sensing for crack detection in a welded stiffener," *Sensors*, vol. 14, no. 7, pp. 12871-12884, 2014, doi: 10.3390/s140712871.
7. B. Masserey and P. Fromme, "In-situ monitoring of fatigue crack growth using high frequency guided waves," *NDT&E Int.*, vol. 71, pp. 1-7, 2015, doi: 10.1016/j.ndteint.2014.12.007.

8. J. R. Gallion and R. Zoughi, "Millimeter-Wave Imaging of Surface-Breaking Cracks in Steel With Severe Surface Corrosion," *IEEE Trans. Instrum. Meas.*, vol. 66, no. 10, pp. 2789-2791, 2017, doi: 10.1109/TIM.2017.2735658.
9. K. M. Donnell, A. McClanahan and R. Zoughi, "On the Crack Characteristic Signal From an Open-Ended Coaxial Probe," *IEEE Trans. Instrum. Meas.*, vol. 63, no. 7, pp. 1877-1879, 2014, doi: 10.1109/TIM.2014.2317295.
10. M. Dvorsky, M. T. A. Qaseer and R. Zoughi, "Detection and Orientation Estimation of Short Cracks Using Circularly Polarized Microwave SAR Imaging," *IEEE Trans. Instrum. Meas.*, vol. 69, no. 9, pp. 7252-7263, 2020, doi: 10.1109/TIM.2020.2978317.
11. F. Li, G. Meng, et al, "Dispersion analysis of Lamb waves and damage detection for aluminum structures using ridge in the time-scale domain," *Meas. Sci. Technol.*, vol. 20, pp. 1-10, 2009, doi: 10.1088/0957-0233/20/9/095704
12. H. Baid, C. Schaal, et al, "Dispersion of Lamb waves in a honeycomb composite sandwich panel." *Ultrasonics*, vol. 56, pp. 409-416, 2015, doi: 10.1016/j.ultras.2014.09.007.
13. P. Wang and Q. Shi, "Damage Identification in Structures Based on Energy Curvature Difference of Wavelet Packet Transform," *Shock & Vibration*, pp. 1-13, 2018, doi: 10.1155/2018/4830391.
14. Q. Wang, Y. Xu, et al, "An Enhanced Time-Reversal Imaging Algorithm-Driven Sparse Linear Array for Progressive and Quantitative Monitoring of Cracks".

- IEEE Trans. Instrum. Meas.*, vol. 68, no. 10, pp. 3433-3445, 2019, doi: 10.1109/TIM.2018.2879071.
15. H. Karami, M. Azadifar, et al, "Single-Sensor EMI Source Localization Using Time Reversal: An Experimental Validation", *Electronics*, 2021, doi: 10.3390/electronics10192448
 16. J. He, C. Zhou, et al, "Research on pipeline damage imaging technology based on ultrasonic guided waves", *Shock Vib.*, vol. 6, pp. 1-18, Jul. 2019, doi: 10.1155/2019/1470761.
 17. Z. Wang, S. Huang, et al, "Multihelical Lamb Wave Imaging for Pipe-Like Structures Based on a Probabilistic Reconstruction Approach," *IEEE Trans. Instrum. Meas.*, vol. 70, pp. 1-10, 2021, doi: 10.1109/TIM.2020.3038474.
 18. J. He, Y. Ran, et al, "A Fatigue Crack Size Evaluation Method Based on Lamb Wave Simulation and Limited Experimental Data," *Sensors*, vol. 17, no. 9, 2017, doi: 10.3390/s17092097.
 19. S. Yuan, J. Chen, et al. "On-line crack prognosis in attachment lug using Lamb wave-deterministic resampling particle filter-based method," *Smart Mater. Struct.*, vol. 26, no. 8, 2017, doi: 10.1088/1361-665X/aa7168.
 20. L. Draudviliene and A. Meškuotienė, "The methodology for the reliability evaluation of the signal processing methods used for the dispersion estimation of Lamb waves," *IEEE Trans. Instrum. Meas.*, 2021, doi: 10.1109/TIM.2021.3127625.

21. V. Giurgiutiu, "Tuned Lamb wave excitation and detection with piezoelectric wafer active sensors for structural health monitoring," *J. Intell. Mater. Syst. Struct.*, 2016, doi: 10.1177/1045389x05050106.
22. L. Chen, Q. Xiao, et al, "A time-of-flight revising approach to improve the image quality of Lamb wave tomography for the detection of defects in composite panels," *Sci. Eng. Compos. Mater.*, vol. 25, pp. 587-592, 2016, doi: 10.1515/secm-2015-0399.
23. Q. Wang and S. Yuan, "Baseline-free imaging method based on new PZT sensor arrangements," *J. Intell. Mater. Syst. Struct.*, vol. 20, no. 14, pp. 1663-1673, 2009, doi: 10.1177/1045389X09105232
24. B. Zhang, X. Hong and Y. Liu, "Deep Convolutional Neural Network Probability Imaging for Plate Structural Health Monitoring Using Guided Waves," *IEEE Trans. Instrum. Meas.*, vol. 70, pp. 1-10, 2021, doi: 10.1109/TIM.2021.3091204.
25. F. Li, H. Peng, and G. Meng, "Quantitative damage image construction in plate structures using a circular PZT array and Lamb waves," *Sens. Actuators A, Phys.*, vol. 214, no.4, pp. 66-73, 2014, doi: 10.1016/j.sna.2014.04.016.
26. S. Wang, W. Wu, et al, "Influence of the PZT Sensor Array Configuration on Lamb Wave Tomography Imaging with the RAPID Algorithm for Hole and Crack Detection." *Sensors*. vol. 20, no. 3, pp. 860, 2020, doi: 10.3390/s20030860.

27. Q. Wang, M. Hong and Z. Su, "An In-Situ Structural Health Diagnosis Technique and Its Realization via a Modularized System," *IEEE Trans. Instrum. Meas.*, vol. 64, no. 4, pp. 873-887, 2015, doi: 10.1109/TIM.2014.2362417
28. B. Sheen and Y. Cho, "A study on quantitative lamb wave tomogram via modified RAPID algorithm with shape factor optimization," *Int. J. Precis. Eng. Man.*, vol.13, no. 5, pp. 671-677, 2012, doi: 10.1007/s12541-012-0087-2.
29. T. R. Hay, R. L. Royer, et al, "A comparison of embedded sensor Lamb wave ultrasonic tomography approaches for material loss detection," *Smart Mater. Struct.*, vol. 15, pp. 946-951, 2006, doi: 10.1088/0964-1726/15/4/007.
30. C. Seong-Won , K. M. Farinholt, et al, "Damage identification of wind turbine blades using piezoelectric transducers," *Shock & Vibration*, pp. 4-7, 2014, doi: 10.1155/2014/430854.